Supplementary Information for:

Reflective Metagrating Polarimeter for Single-Shot Full Stokes Mapping: Toward Digital Histopathology

Paul Thrane[1,2,†,*], Chao Meng[1,†,*], Alexander Bykov[3], Oleksii Sieryi[3], Fei Ding[1], Igor Meglinski[4], Christopher A. Dirdal[2] and Sergey I. Bozhevolnyi[1,*]

[1] Centre for Nano Optics, University of Southern Denmark, Campusvej 55, DK-5230 Odense, Denmark.

[2] Smart Sensors and Microsystems, SINTEF Digital, Gaustadalleen 23C, 0373 Oslo, Norway.

[3] OPEM, ITEE, University of Oulu, 90014 Oulu, Finland.

[4] College of Engineering and Physical Sciences, Aston University, Birmingham B4 7ET, U.K.

† These authors contributed equally.

* paul.thrane@sintef.no

* chao@mci.sdu.dk

* seib@mci.sdu.dk

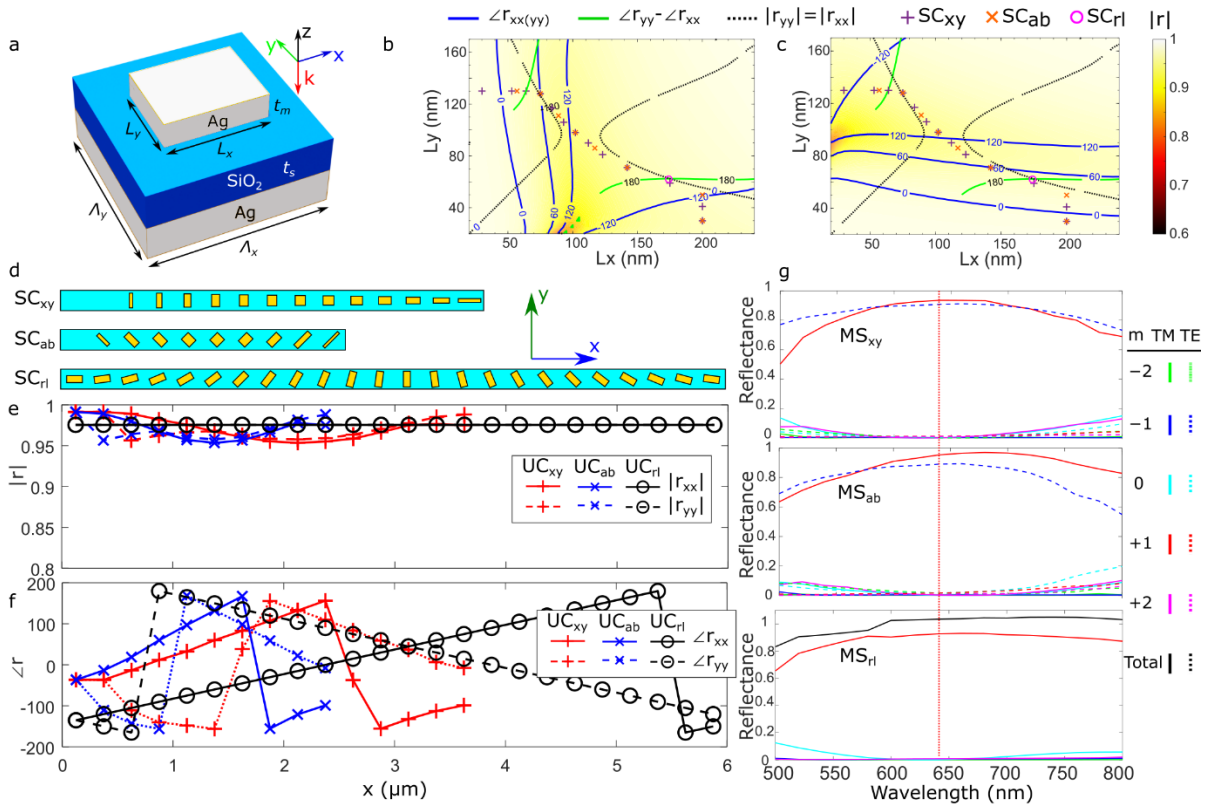

Fig. S1. MS polarimeter grating design based on silver nanostructures. In the main text, the fabricated MS polarimeter was based on gold nanostructures, but as can be seen in this figure, switching to silver would enable high efficiency polarimetric measurements also for shorter wavelengths. **a** Schematic of a unitcell. **b** and **c** are reflection amplitudes for light linearly polarized light normally incident on a periodic unitcell with nanobrick dimensions L_x and L_y, for a wavelength of 640 nm. **d** is a drawing of the periodic cells used to make the three supercells. **e** and **f** are the reflection amplitudes and phases for the chosen geometries, while the plots in **g** are the simulated diffraction order efficiencies for the three diffraction gratings before being interleaved.

Supplementary Note

In the main text we present a method of using two 4×6 matrices to do the MS polarimeter calibration, which was found to give the best results. Here we present the initial procedure we investigated which uses a single 3x6 calibration matrix $\boldsymbol{M}$, determined by measuring the diffraction patterns for a set of n known polarization states

$$\boldsymbol{S} = \begin{pmatrix} s_{1,1} & \cdots & s_{1,n} \\ s_{2,1} & \cdots & s_{2,n} \\ s_{3,1} & \cdots & s_{3,n} \end{pmatrix} = \boldsymbol{MI} = \boldsymbol{M} \begin{pmatrix} I_{x,1}/(I_{x,1}+I_{y,1}) & \cdots & I_{x,n}/(I_{x,n}+I_{y,n}) \\ I_{y,1}/(I_{x,1}+I_{y,1}) & \cdots & I_{y,n}/(I_{x,n}+I_{y,n}) \\ I_{a,1}/(I_{a,1}+I_{b,1}) & \cdots & I_{a,n}/(I_{a,n}+I_{b,n}) \\ I_{b,1}/(I_{a,1}+I_{b,1}) & \cdots & I_{b,n}/(I_{a,n}+I_{b,n}) \\ I_{r,1}/(I_{r,1}+I_{l,1}) & \cdots & I_{r,n}/(I_{r,n}+I_{l,n}) \\ I_{l,1}/(I_{r,1}+I_{l,1}) & \cdots & I_{l,n}/(I_{r,n}+I_{l,n}) \end{pmatrix}$$

Here $s_{i,j}$ is the i^{th} stokes parameter of the j^{th} polarization state, and $I_{i,j}$ is the intensity in diffraction order i of the j^{th} polarization state. The calibration matrix can then be calculated by $\boldsymbol{M} = \boldsymbol{SI}^{+}$, with $\boldsymbol{I}^{+}$being the pseudoinverse of $\boldsymbol{I}$. Any unknown polarization state can then be determined using the measured diffraction intensities and $\boldsymbol{M}$ as

$$S_{\text{calibrated}} = \boldsymbol{M} \begin{pmatrix} I_x/(I_x+I_y) \\ I_y/(I_x+I_y) \\ I_a/(I_a+I_b) \\ I_b/(I_a+I_b) \\ I_r/(I_r+I_l) \\ I_l/(I_r+I_l) \end{pmatrix}$$

The results are shown in Supplementary Figures S2-S4.

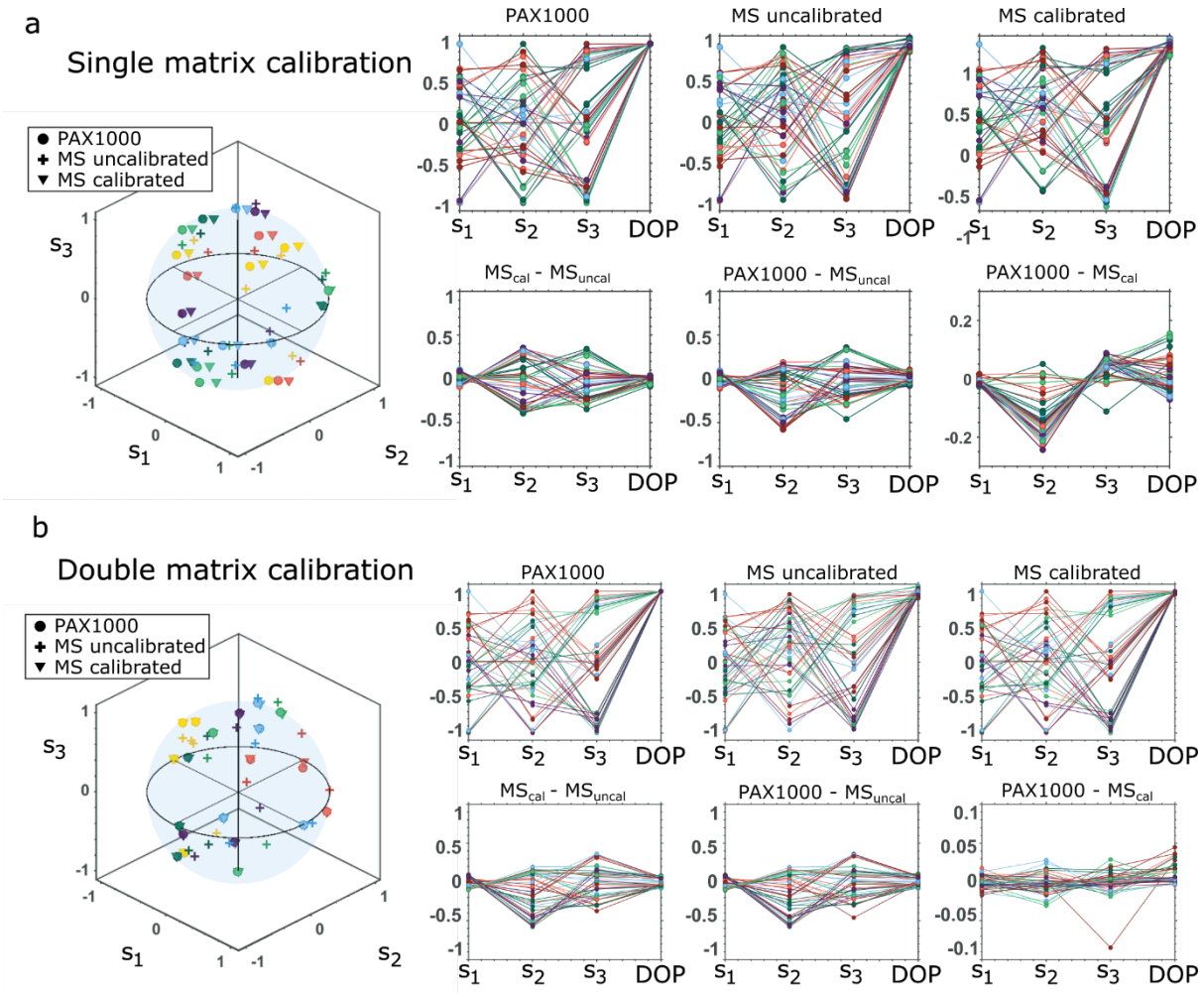

Fig. S2. Characterization of the MS polarimeter with fully polarized light. **a** Calibration results when using a single calibration matrix. **b** Calibration results shown in Figure 4 in the main text, done using two calibration matrices. When comparing the two plots labeled "PAX1000 – MS_{cal}" it is obvious that the S_2 measurements are skewed when using a single matrix. This is due to an asymmetric design of SC_{ab}, which is why we chose to use two separate matrices for when $S_2 \geq 0$ and $S_2 < 0$.

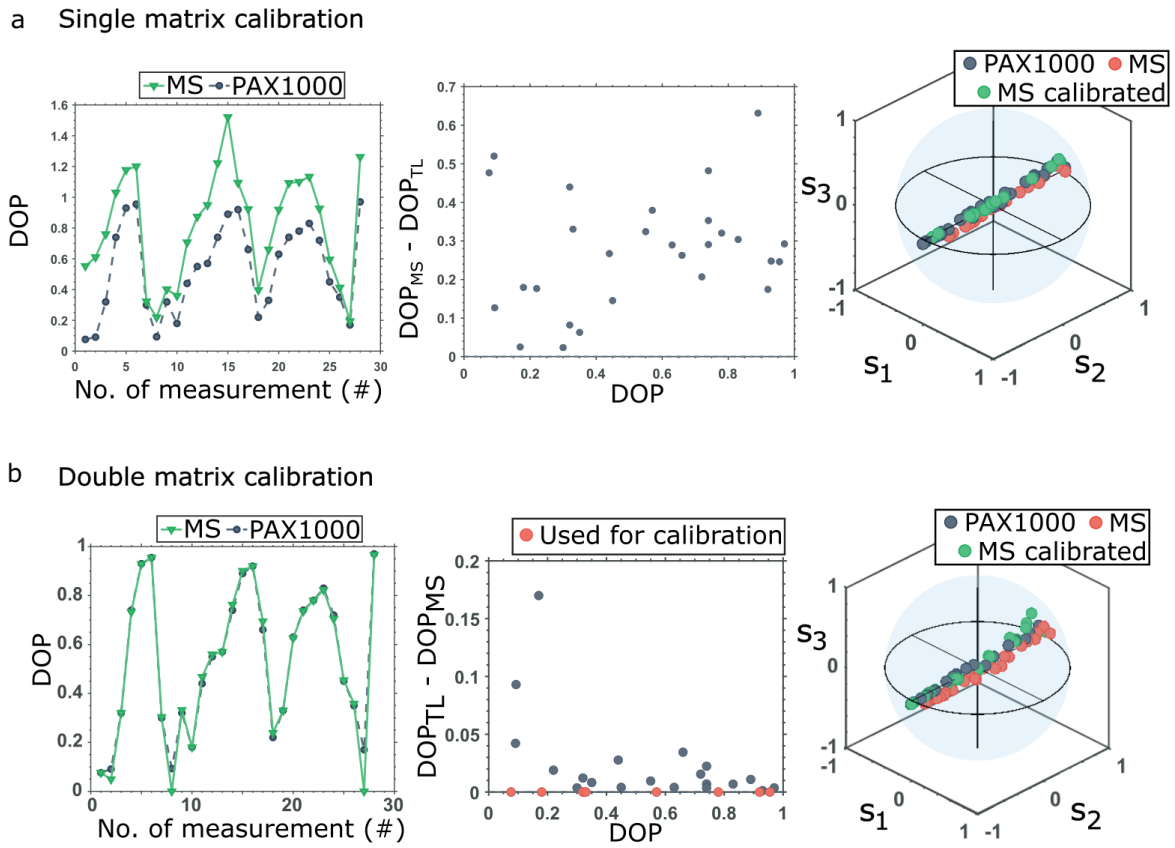

Fig. S3. Characterization of the MS polarimeter with partially polarized light. **a** Calibration results when using a single calibration matrix. **b** Calibration results when using two matrices and adding a row in the calibration matrices for adjusting the DOP, as presented in Figure 5 of the main text. Notice that the DOP is clearly wrong for the single matrix method, with the DOP > 1 for several measurements calculated as the norm of the three Stokes parameters. In a all the measurement points have been included in the calibration, while for the plots in b only a subset have been used – as indicated by red dots in the middle plot.

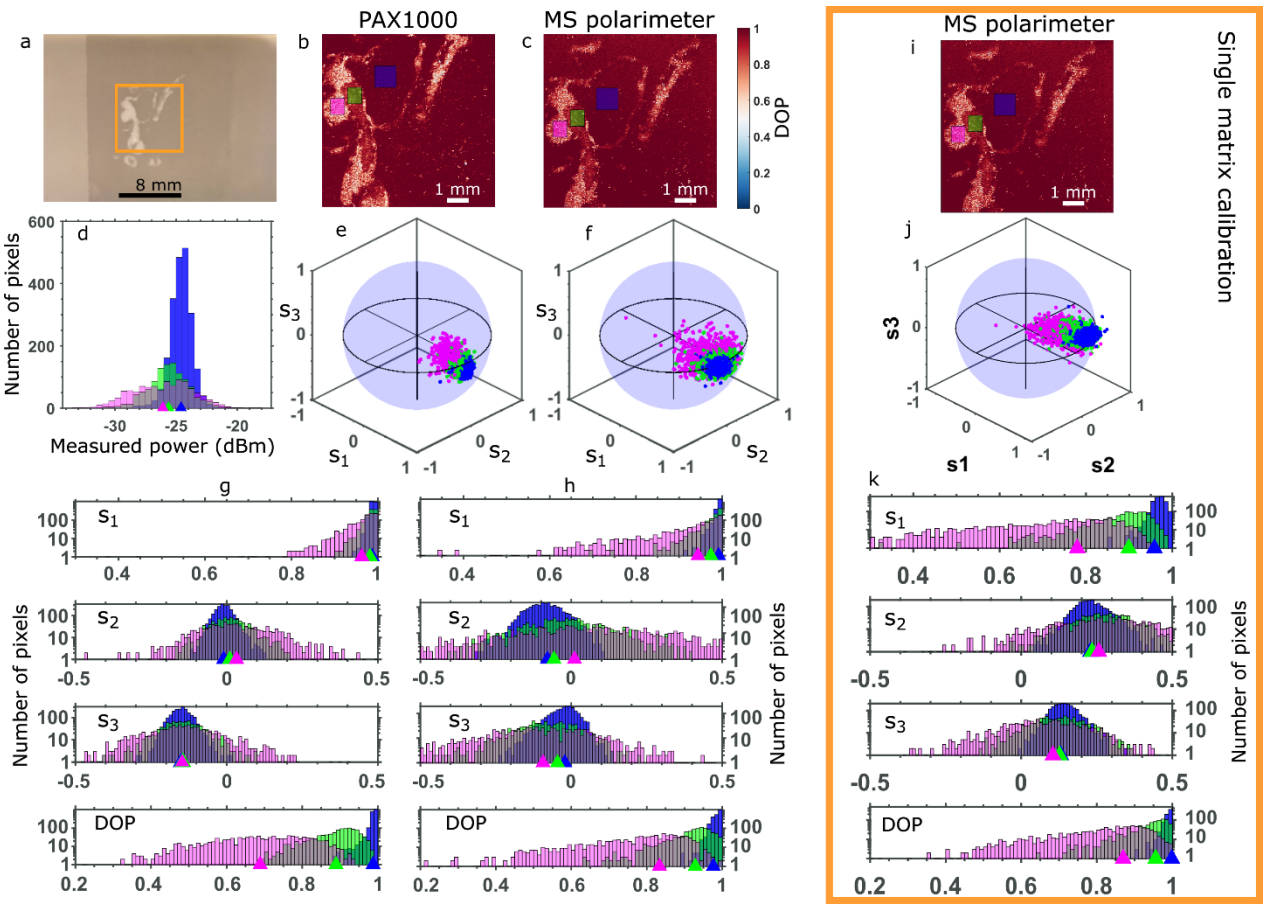

Fig. S4. Benchmarking with tissue phantom. **a-h** Benchmarking results presented in Figure 6 of the main text. **i-k** Benchmarking results when using a single calibration matrix. As mentioned in Figure S2, when using a single calibration matrix the S_2 measurement is skewed which can be seen as a shift in S_2 towards positive values. Including the calibration for the DOP also improves the S_1 and S_3 measurements, even though the calibration matrices were constructed using only polarization states with DOP = 1. Adding partially polarized light to the calibration procedure is expected to improve the results.

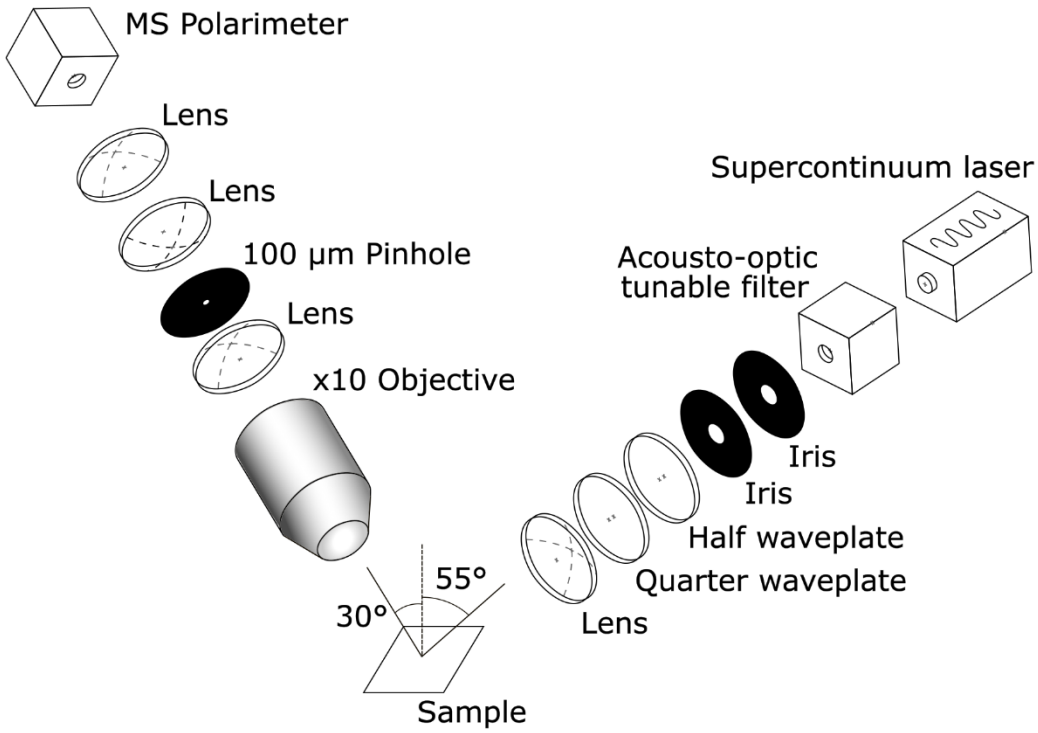

Fig. S5. Setup for benchmarking of MS polarimeter. Schematic of the setup used to characterize the MS polarimeter. Light from a supercontinuum laser is wavelength-filtered and passes through polarization controlling optics to ensure a circular polarized beam is focused onto the sample. A microscope objective is used to collect light scattered at a non-specular direction and passed through a pinhole before being measured by the polarimeter. The sample is placed on a 2-axis translation stage to scan the focal point across the sample. The measurement is done twice, once with the MS polarimeter and once with the reference polarimeter (Thorlabs PAX1000). The setup is described further in [Ivanov, D. *et al.* Polarization-Based Histopathology Classification of Ex Vivo Colon Samples Supported by Machine Learning. *Frontiers in Physics* **9**, 814787 (2022)] and [Ivanov, D. *et al.* Polarization and depolarization metrics as optical markers in support to histopathology of ex vivo colon tissue. *Biomedical Optics Express* **12**, 4560 (2021)].

Table S1. An overview of metasurface based polarization measurement systems.

Title	First author	Year	Integrated	Application	Comment	Link
Plasmonic metagratings for simultaneous determination of Stokes parameters	Pors	2015	No	Stokes polarimetry	Polarization splitting grating	http://dx.doi.org/10.1364/OPTICA.2.000716
Ultracompact metasurface in-line polarimeter	Mueller	2016	No	Stokes polarimetry	In-plane polarization sensitive scattering	http://dx.doi.org/10.1364/OPTICA.3.000042
Waveguide Metacouplers for In-Plane Polarimetry	Pors	2016	No	Stokes polarimetry	Polarization dependent generation of SPP	http://dx.doi.org/10.1103/PhysRevApplied.5.064015
On-Chip Optimal Stokes Nanopolarimetry Based on Spin–Orbit Interaction of Light	Espinosa-Soria	2017	No	Stokes polarimetry	Polarization dependent coupling into waveguides	http://dx.doi.org/10.1021/acs.nanolett.7b00564
Performance characteristics of 4-port in-plane and out-of-plane in-line metasurface polarimeters	Juhl	2017	No	Stokes polarimetry	Polarization splitting grating	https://doi.org/10.1364%2FOE.25.028697
Visible Metasurfaces for On-Chip Polarimetry	Wu	2017	No	Stokes polarimetry	Polarization splitting grating	http://dx.doi.org/10.1021/acsphotonics.7b01527
Full-Stokes Imaging Polarimetry Using Dielectric Metasurfaces	Arbabi	2018	No	Stokes polarimetry	Polarization splitting grating	http://dx.doi.org/10.1021/acsphotonics.8b00362
Polarimetry Using Graphene-Integrated Anisotropic Metasurfaces	Jung	2018	No	Stokes polarimetry	Modulated polarization sensitive reflection into photodetector.	http://dx.doi.org/10.1021/acsphotonics.8b01216
Polarization state generation and measurement with a single metasurface	Rubin	2018	No	Stokes polarimetry	Polarization splitting grating	https://doi.org/10.1364/OE.26.0214
Ultracompact Broadband Plasmonic Polarimeter	Lee	2018	No	Stokes polarimetry	Polarization dependent generation of SPP	https://doi.org/10.1002%2Flpor.201700297
Chip-integrated plasmonic flat optics for mid-infrared full-Stokes polarization detection	Bai	2019	No	Stokes polarimetry	Polarization conversion then filtering	https://doi.org/10.1364/PRJ.7.001051
Multifunctional geometric phase optical element for high-efficiency full Stokes imaging polarimetry	Dai	2019	No	Stokes polarimetry	Polarization splitting grating	https://doi.org/10.1364/PRJ.7.001066
Nature-inspired chiral metasurfaces for circular polarization detection and full-Stokes polarimetric measurements	Basiri	2019	No	Stokes polarimetry	Polarization conversion then filtering	https://doi.org/10.1038%2Fs41377-019-0184-4
Polarimetry with Disordered Photonic Structures	Juhl	2019	No	Stokes polarimetry	Neural network and polarization dependent scattering	http://dx.doi.org/10.1021/acsphotonics.9b01420
Full Stokes Polarimetry for Wide-Angle Incident Light	Zhang	2020	No	Stokes polarimetry	Polarization splitting grating	https://doi.org/10.1002%2Fpssr.202000044
Monolithic Full-Stokes Near-Infrared Polarimetry with Chiral Plasmonic Metasurface Integrated Graphene–Silicon Photodetector	Li	2020	Yes	Stokes polarimetry	Polarization sensitive detector	https://pubs.acs.org/doi/10.1021/acsnano.0c00724?ref=pdf
Full-Stokes Polarimeter Based on Chiral Perovskites with Chirality and Large Optical Anisotropy	Ma	2021	Yes	Stokes polarimetry	Polarization sensitive detector	https://doi.org/10.1002/smll.202103855
High efficiency all-dielectric pixelated metasurface for near-infrared full-Stokes polarization detection	Zhang	2021	No	Stokes polarimetry	Polarization filters	https://doi.org/10.1364/PRJ.415342
An All-Dielectric Metasurface Polarimeter	Shah	2022	No	Stokes polarimetry	MS grating	https://doi.org/10.1021/acsphotonics.2c00395
Full-Stokes polarimetry based on rotating metasurfaces	Gong	2022	No	Stokes polarimetry	Rotating MS	https://doi.org/10.1063/5.0078097
Full-Stokes Polarimetry for Visible Light Enabled by an All-Dielectric Metasurface	Ren	2022	No	Stokes polarimetry	Polarization splitting grating	https://doi.org/10.1002%2Fadpr.202100373
A silicon metasurface for full-Stokes polarimetry of infrared light	Ren	2023	No	Stokes polarimetry	Grating with integrated focusing	https://doi.org/10.1063/5.0140858
Evaluation and characterization of imaging polarimetry through metasurface polarization gratings	Li	2023	No	Stokes polarimetry	Benchmarking test.	https://opg.optica.org/abstract.cfm?URI=ao-62-7-1704
Highly Precise and Broadband Full-Stokes Polarimeter Based on a Deep Learning Algorithm	Xian	2023	No	Stokes polarimetry	Anisotropic structures then mapping behavior with machine learning	https://doi.org/10.1021/acsphotonics.3c00007
Tunable Far-Infrared Polarization Imaging Based on VO2 Metasurfaces	Ma	2023	No	Stokes polarimetry	Active MS instead of rotating polarization filter	https://advanced.onlinelibrary.wiley.com/doi/10.1002/adom.202302390
Realizing Minimally Perturbed, Nonlocal Chiral Metasurfaces for Direct Stokes Parameter Detection	Ki	2024	No	Stokes polarimetry	Polarization dependent transmission from nonlocal effect	https://pubs.acs.org/doi/10.1021/acsnano.3c10749
Robust Classical and Quantum Polarimetry with a Single Nanostructured Metagrating	Lung	2024	No	Stokes polarimetry	Polarization splitting grating, alternative optimization	https://pubs.acs.org/doi/10.1021/acsphotonics.3c01287?ref=pdf
Integrated plasmonic metasurfaces for spectropolarimetry	Chen	2016	No	Spectropolarimetry	Polarization splitting grating	http://dx.doi.org/10.1088/0957-4484/27/22/224002
Beam-Size-Invariant Spectropolarimeters Using Gap-Plasmon Metasurfaces	Ding	2017	No	Spectropolarimetry	Polarization splitting grating	http://dx.doi.org/10.1021/acsphotonics.6b01046
Computational spectropolarimetry with a tunable liquid crystal metasurface	Ni	2022	No	Spectropolarimetry	Liquid crystal adjustable, with computational reconstruction	https://elight.springeropen.com/articles/10.1186/s43593-022-00032-0
Spinning metasurface stack for spectro-polarimetric thermal imaging	Wang	2023	Yes	Spectropolarimetric thermal imaging	Spinning waveplates	https://opg.optica.org/abstract.cfm?URI=optica-11-1-73
Multispectral and polarimetric photodetection using a plasmonic metasurface	Pelzman	2018	Yes	Spectral linear polarization measurement	Polarization-spectral filter on detector array	https://pubs.aip.org/aip/jap/article/123/4/043107/347091/Multispectral-and-polarimetric-photodetection
An Ultra-Broadband High Efficiency Polarization Beam Splitter for High Spectral Resolution Polarimetric Imaging in the Near Infrared	Hsiao	2022	Yes	Polarization beam splitter	For NIR spectropolarimetric telescope	https://doi.org/10.1002%2Fadvs.202201227
Generalized Hartmann-Shack array of dielectric metalens sub-arrays for polarimetric beam profiling	Yang	2018	No	Polarimetric beam profiling	Array of polarization splitting gratings	https://doi.org/10.1038%2Fs41467-018-07056-6
Metasurface Polarimeter on Optical Fiber Facet by Nano-Transfer to UV-Curable Hybrid Polymer	Juhl	2019	Yes	Optical fiber	Grating on fiber facet	https://doi.org/10.1109%2FJSTQE.2019.2893757
Compact and scalable polarimetric self-coherent receiver using a dielectric metasurface	Soma	2023	Yes	Optical fiber	Attaching MS to fiber and aligning with detector array	https://opg.optica.org/abstract.cfm?URI=optica-10-5-604
Broadband Single-Chip Full Stokes Polarization-Spectral Imaging Based on All-Dielectric Spatial Multiplexing Metalens	Sun	2022	No	NIR polarization-spectral imaging	Spatial multiplexing metalens	https://onlinelibrary.wiley.com/doi/10.1002/lpor.202100650
Switchable Unipolar-Barrier Van der Waals Heterostructures with Natural Anisotropy for Full Linear Polarimetry Detection	Deng	2022	Yes	Linear polarization detection	Polarization sensitive detector	https://doi.org/10.1002%2Fadma.202203766
Angle-Resolved Polarimetry with Quasi-Bound States in the Continuum Plasmonic Metamaterials via 3D Aerosol Nanoprinting	Yang	2024	No	Linear polarization and angle detection	Scattering from polarization and angle sensitive antennae	https://pubs.acs.org/action/showCitFormats?doi=10.1021/acsnano.3c12024&ref=pdf
Matrix Fourier optics enables a compact full-Stokes polarization camera	Rubin	2019	Yes	Imaging	Spatial multiplexing metalens	http://dx.doi.org/10.1126/science.aax1839
Compound-eye metasurface optics enabling a high-sensitivity, ultra-thin polarization camera	Miyata	2020	No	Imaging	Spatial multiplexing metalens	https://doi.org/10.1364/OE.389591
Crosstalk-free achromatic full Stokes imaging polarimetry metasurface enabled by polarization-dependent phase optimization	Zhang	2022	No	Imaging	Spatial multiplexing metalens	https://doi.org/10.29026/oea.2022.220058
Imaging polarimetry through metasurface polarization gratings	Rubin	2022	Yes	Imaging	Grating in front of imaging system	https://opg.optica.org/abstract.cfm?URI=oe-30-6-9389
Chip-integrated metasurface full-Stokes polarimetric imaging sensor	Zuo	2023	Yes	Imaging	Pixel polarization filter	https://www.nature.com/articles/s41377-023-01260-w
Disordered metasurface enabled single-shot full-Stokes polarization imaging leveraging weak dichroism	Fan	2023	No	Imaging	Filter on sensor combined with reconstruction algorithm	https://doi.org/10.1038/s41467-023-42944-6
High-Resolution Metalens Imaging Polarimetry	Huang	2023	No	Imaging	Spatial multiplexing metalens	https://doi.org/10.1021/acs.nanolett.3c03258
Neural network assisted high-spatial-resolution polarimetry with non-interleaved chiral metasurfaces	Chen	2023	No	Imaging	Other multiplexing technique	https://www.nature.com/articles/s41377-023-01337-6
Non-Line-of-Sight Full-Stokes Polarimetric Imaging with SolutionProcessed Metagratings and Shallow Neural Networks	Weng	2023	No	Imaging	Polarization dependent scattering and neural network	https://pubs.acs.org/doi/10.1021/acsphotonics.3c00291?ref=pdf
Single-shot wide-field full-stokes polarization imaging	Li	2024	No	Imaging	Spatial multiplexing metalens	https://linkinghub.elsevier.com/retrieve/pii/S0143816623003895
Flat, wide field-of-view imaging polarimeter	Li	2025	Yes	Imaging	Spatial multiplexing metalens	https://opg.optica.org/optica/fulltext.cfm?uri=optica-12-6-799&id=572531
All-dielectric metasurface for fully resolving arbitrary beams on a higher-order Poincaré sphere	Yang	2021	No	Higher order poincare sphere measurement	Polarization splitting grating	https://doi.org/10.1364/PRJ.411503
Metasurface higher-order poincaré sphere polarization detection clock	Yang	2025	No	Higher order poincare sphere measurement	Other multiplexing technique	https://www.nature.com/articles/s41377-024-01738-1
Metasurface-Enabled 3-in-1 Microscopy	Intaravanne	2023	No	Chiral polarimetry and edge detection	Polarization sensitive metasurface in Fourier plane	https://pubs.acs.org/doi/full/10.1021/acsphotonics.2c01971
Ultrathin circular polarimeter based on chiral plasmonic metasurface and monolayer $MoSe_2$†	Jiang	2020	Yes	Chiral polarimetry	Polarization sensitive detector	https://doi.org/10.1039/c9nr10768a
Highly Efficient Anisotropic Chiral Plasmonic Metamaterials for Polarization Conversion and Detection	Bai	2021	No	Chiral polarimetry	Polarization conversion then filtering	https://doi.org/10.1021/acsnano.1c02278?urlappend=%3Fref%3DPDF&jav=VoR&rel=cite-as
Monocular metasurface camera for passive single-shot 4D imaging	Shen	2023	Yes	3D and polarimetric imaging	Polarization and angle dependent point spread function	https://www.nature.com/articles/s41467-023-36812-6

Table S2. Key performance characteristics of state-of-the-art systems capable of full-Stokes polarimetry compared with a commercially available polarimeter.

	Principle	Wavelength (nm)	Speed	Partial polarization	Optical pathlength	Minimum possible size	Demonstrated application	Fabrication scalability
Thorlabs PAX 1000	Rotating QWP and linear polarizer	VIS/NIR/IR	400 Hz	Yes	~3 cm	~4 cm	Clinical imaging	Poor
Ref 20	3 interleaved dielectric gratings	1550	10 GHz	No	~1.5 cm	~5 mm	Fiberoptic-communication	Good
Ref 33	6 polarization filters	630-670; 480-520	30 Hz	Yes	<1 mm	~1 mm	Imaging	Good
Ref 41	Graphene-silicon metasurface detector	1550	140 kHz	No	N/A	~1 mm	Polarization sensitive detector	Poor
Ref 42	Chiral perovskite detector	512	11 Hz	No	N/A	~1 mm	Polarization sensitive detector	Poor
Ref 45	Polarization splitting lens	870	56 Hz	No	~2 cm	3 mm	Imaging	Good
This work	**3 interleaved plasmonic gratings**	**640**	**600 Hz**	**Yes**	**~2 cm**	**~5 mm**	**Clinical Imaging**	**Good**

Table S3. Nanobrick dimensions used for the three super-cells, in nm. For SC_{xy} the format is [L_x,L_y], while for SC_{ab} the nanobricks have been rotated by 45°. For SC_{rl} 24 nanobricks with the same dimensions are used, but each one rotated by 180° divided by 24 compared to its neighbor.

SC_{xy}	SC_{ab}	SC_{rl}
[0,0]	[0,0]	[142,63]
[0,0]	[32,130]	
[30,130]	[60,130]	
[48,130]	[74,109]	
[61,118]	[84,97]	
[71,108]	[93,88]	
[78,100]	[103,79]	
[84,94]	[120,68]	
[90,88]	[171,49]	
[96,82]	[181,24]	
[103,76]		
[112,69]		
[124,59]		
[144,46]		